

Thermally Driven Microvalve with Buckling Behavior for Pneumatic Applications

T. Lisec, H. J. Quenzer, M. Kreutzer, S. Hoerschelmann,
B. Wagner and W. Benecke¹

Fraunhofer-Institute for Silicon Technology (FhG-ISiT)
Dillenburger Str. 53, D-14199 Berlin, Germany

¹University of Bremen, Institute of Micro-Sensors, -Actuators and -Systems (IMSAS)
Kufsteiner Straße, Postfach 330 440, D-28334 Bremen, Germany

(Received November 4, 1994; accepted December 4, 1995)

Key words: silicon microvalve, thermomechanical actuation, thermally induced buckling

We present theoretical and experimental results of a new thermally driven microvalve. In contrast to earlier reported devices with bimorph composition this valve is based on the buckling effect of a heated pure silicon bridge structure. Simulation, fabrication and experimental results are presented. Theoretical and finite-element analysis (FEA) of the thermomechanical behavior are performed. Prototypes of this initial valve design operate with inlet pressures up to 1.0 bar showing flow rates of more than 700 ml/min. The measured switching time is about 15 ms which is extremely quick for thermal actuators. The power consumption of this valve is between 1 and 4 W.

1. Introduction

Gas and fluid control systems are one of the most important applications for silicon actuators. For the actuation mechanism of microvalves electrostatic,^(1,2) thermomechanic,⁽³⁾ piezoelectric⁽⁴⁾ or magnetic principles⁽⁵⁾ have been used. Magnetic and piezoelectric drives require the hybrid integration of magnets⁽⁶⁾ or piezodiscs to achieve large deflections. Electrostatic excitations can easily be integrated monolithically. However, the actuation distance is limited due to the short-range force. More sophisticated electrostatic concepts use S-shaped⁽⁷⁾ or prebuckled electrodes.⁽⁸⁾

Based on thermal principles both high forces and large deflections can be generated in

a simple manner. The first complete thermally driven valve, containing an electrically actuated bimorph diaphragm,⁽⁹⁾ provides control of gas flow up to 150 ml/min in a pressure range up to 3.5 bar. The required input power is lower than 0.5 W, but the response time is too long for switching applications.

The objective of the present work is the development of a pneumatic switching microvalve for high gas flow and short response time. A thermal driving method using the buckling effect of a silicon microbridge was chosen.

2. Basic Valve Structure

The microvalve consists of two $5 \times 5 \times 0.5 \text{ mm}^3$ silicon chips. A schematic cross-sectional view of the valve is given in Fig. 1. The lower active chip contains a cross-shaped membrane structure ($2600 \times 2600 \mu\text{m}^2$ total area) with n^+ -doped polysilicon heaters and gold metal lines. Each arm of the structure has a width of $600 \mu\text{m}$. The upper passive chip contains the valve seat ($80 \mu\text{m}$ width) with the orifice ($360 \times 360 \mu\text{m}^2$). Figure 2 shows top views of both chips. The valve is normally closed. Compared to a closed diaphragm the four-sided suspension has a better thermal decoupling from the frame.

3. Thermally Induced Buckling

A mechanically bistable bridge with intrinsic compressive stress has been discussed extensively.⁽¹⁰⁾ Thermally induced buckling of a silicon beam has already been described.⁽¹¹⁾ The mechanism may be explained with reference to the double-clamped silicon bridge with integrated heaters shown in Fig. 3. Heating causes an expansion of the membrane structure while the colder silicon frame remains fixed on the substrate. The resulting high compressive strain within the membrane accumulates up to a critical value.

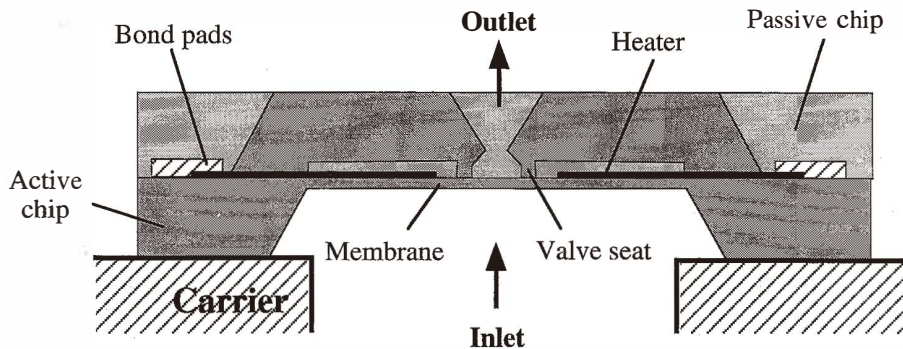


Fig. 1. Cross-sectional view of a valve.

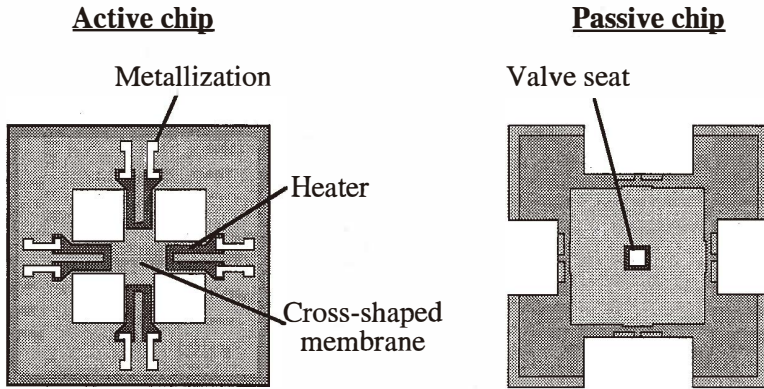


Fig. 2. Top view of both chips.

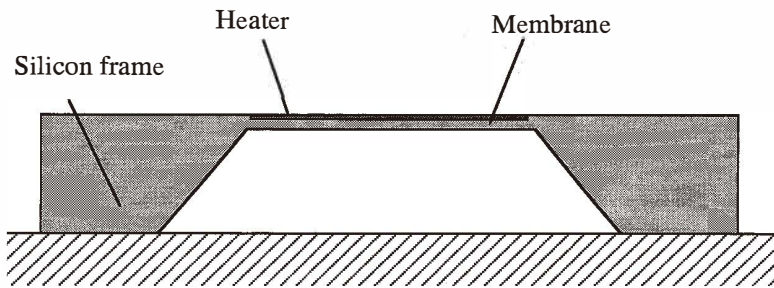


Fig. 3. Basic silicon structure of the valve.

If this maximum load is exceeded, the membrane buckles instantly. The membrane structure integrated in the valve in Fig. 1 can move only downward due to the presence of the valve seat.

In the case of a rigidly clamped beam, the critical buckling strain (Euler load) can be determined from the following equation:⁽¹⁰⁾

$$\epsilon_{crit} = \frac{\pi^2}{3} \cdot \frac{t^2}{l^2}, \tag{1}$$

- with t : thickness of the beam
- l : length of the beam
- ϵ_{crit} : critical buckling strain.

This strain can be generated by the temperature difference ΔT between the membrane and the surrounding silicon frame

$$\varepsilon = \frac{\sigma}{E} = \alpha \cdot \Delta T. \quad (2)$$

α : thermal expansion coefficient
 σ : mechanical stress
 E : Young's modulus

From this, the critical buckling temperature between the beam and the frame can be determined as

$$\Delta T_{\text{crit}} = \frac{\pi^2 \cdot t^2}{3\alpha \cdot l^2}. \quad (3)$$

The central deflection of the silicon bridge is approximated by

$$d = \frac{2}{\pi} \cdot l \cdot \sqrt{\alpha \cdot (\Delta T - \Delta T_{\text{crit}})}. \quad (4)$$

The external load which the buckled beam can withstand is given by

$$F = 11 \cdot \sqrt{(\sigma \cdot E)} \cdot \frac{w \cdot t^3}{l^2} \quad (5)$$

$$\text{if } \frac{\sigma}{E} \gg \frac{t^2}{l^2},$$

where w : width of the beam
 t : thickness of the beam
 l : length of the beam.

For the silicon bridge with a thickness of 12 μm and a length of 2.6 mm used in our device, a critical temperature difference of 27°C is calculated. A temperature difference of $\Delta T = 200^\circ\text{C}$ leads to a deflection of 35 μm . For a 600- μm -wide silicon bridge a force of 6 mN is calculated. Consequently, for a four-sided clamped structure, 12 mN can be assumed.

4. Finite Element Analysis

In simulations of the microvalve, ANSYS software implemented on a DEC station 5000/200 was used. Both thermal and mechanical behaviors of the microvalves were simulated.

In the first approach, a simple model of a cross-shaped rigidly clamped silicon

membrane was calculated. Nonlinearities such as large deflection and stress stiffening were considered. Figure 4 shows the buckled FEA structure with a constant temperature of 200°C. The finite-element results indicate that eqs. (3) and (4) for the buckling temperature and the deflection, respectively, are good approximations. However, the calculated force in FEA was about 65% higher than that predicted by eq. (5). For the calculation of the switching pressure (structural simulation), it was assumed that the total inlet pressure acts on the membrane in both orifice and valve seat areas ($520 \times 520 \mu\text{m}^2$). A pressure of nearly 0.9 bar is necessary to switch this structure to the opposite state (Fig. 5).

In an extended model, using an elastic clamp at the silicon frame, the anisotropy of Young's modulus of monocrystalline silicon and the temperature dependence of the coefficient of thermal expansion were integrated. Figure 6 shows the complete model with a uniformly heated membrane (200°C). A pressure load of 0.7 bar is applied from below. In the model with elastic clamping a critical pressure of 0.7 bar is calculated compared with 0.9 bar for rigid clamping.

For the thermal simulations, the temperature dependences of the heat conductivity and thermal capacity as well as the effect of free convection were considered. Temperature distributions over the silicon chip and the thermal time constants for heating and cooling

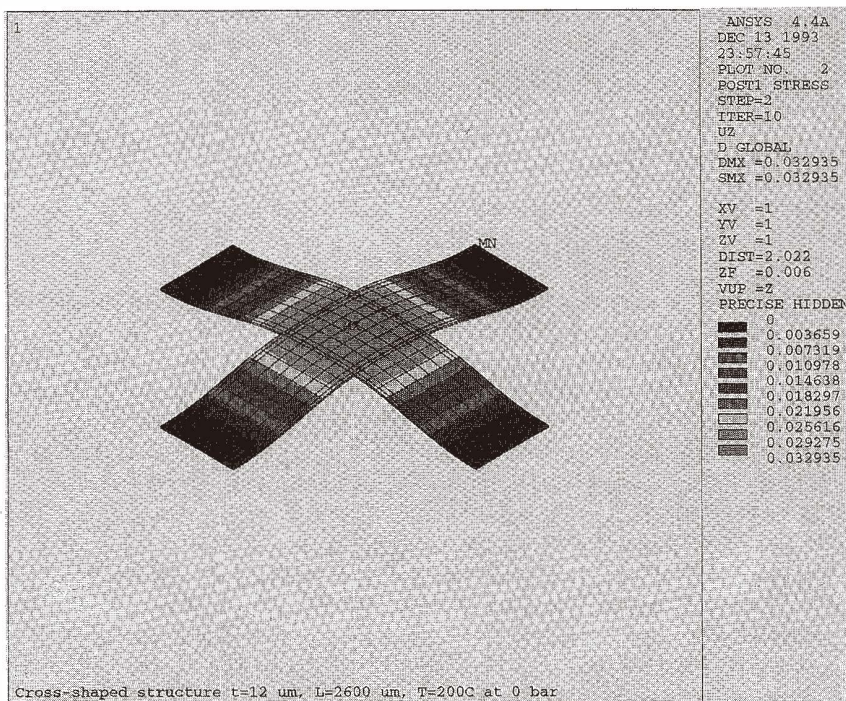


Fig. 4 Buckling of a rigidly clamped membrane structure at a constant temperature of 200°C.

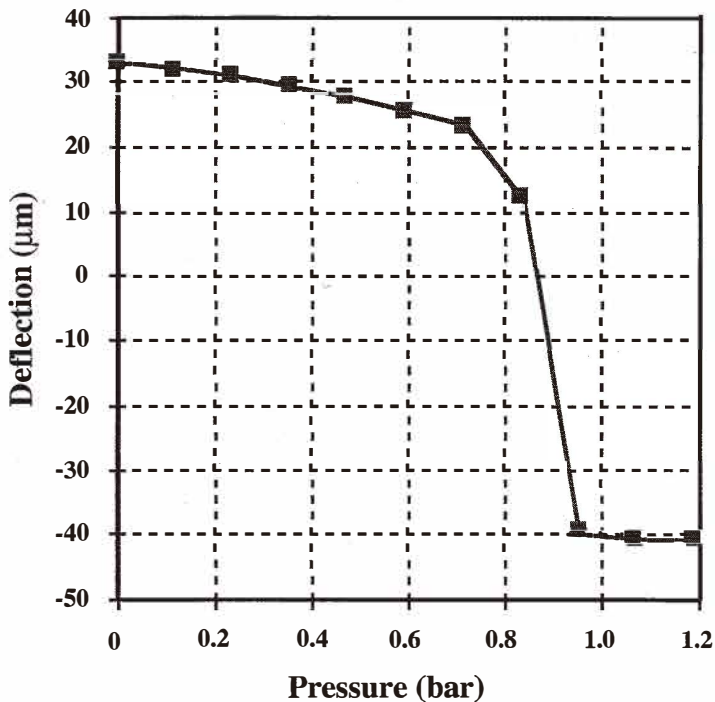


Fig. 5. FEA deflection of a membrane structure vs. applied pressure at a temperature of 200°C.

were determined.

Figure 7 shows the temperature-time characteristics in the center of the membrane heated with three successive pulses each for 30 ms at 1 W, 2 W and 3 W. In Fig. 8 the temperature distribution across the chip for heating power of 1 W is plotted. Near the clamping position, a strong gradient exists. In the center part of the membrane the temperature is slightly reduced due to the free convection.

The thermal behavior of the structure depends strongly on the thickness of the epoxy layer between the active chip and the carrier. For all thermal simulations a thickness value of 50 μm , which was measured in actual devices has been used.

Temperature distributions, obtained for short heating pulses, were then used in structural simulations to determine the maximum pressure which the membrane can withstand at a given heat condition. Such a steady-state calculation roughly correlates to the initiation of the valve opening process before gas flow. For this case the simulated and experimental data obtained may be comparable, even though the valve seat chip has not been considered in the FEA model. For example, at 1.2 W and 30 ms of heating, the simulation gives a temperature of nearly 130°C in the center of the membrane and a reversible pressure of 0.15 bar.

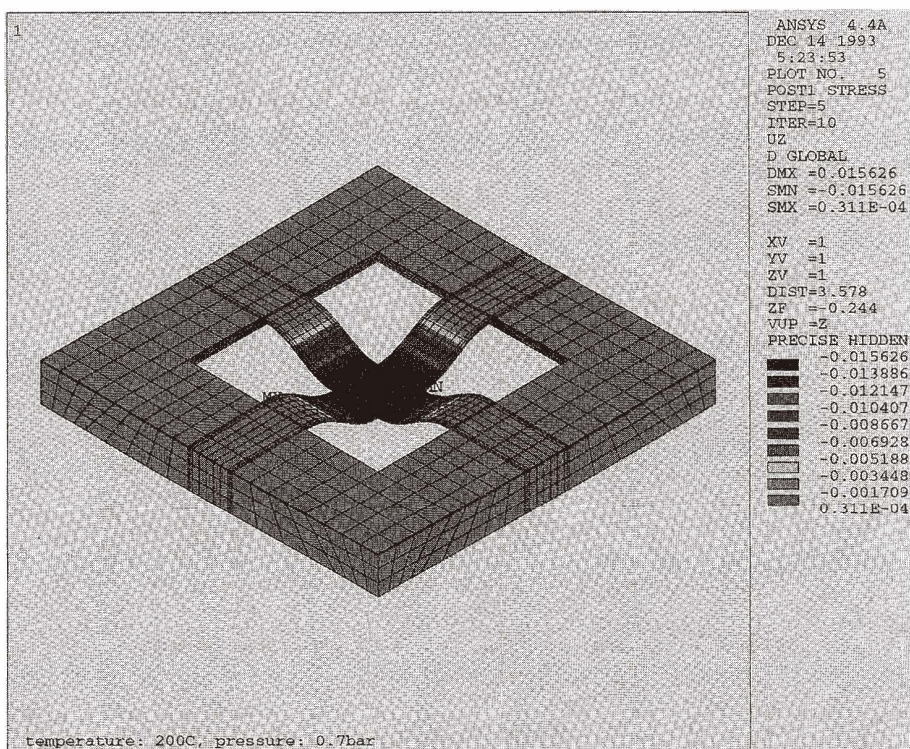


Fig. 6. Deflection of a membrane structure at a temperature of 200°C against an applied pressure of 0.7 bar (from below).

5. Fabrication

For fabrication of the valve, double-sided polished 525- μm -thick silicon wafers were used. The entire process requires 7 lithographic masks for both chips.

First, polysilicon heaters were patterned on an oxidized substrate. By means of phosphorous doping a resistance between 10 and 20 Ω/square for polysilicon thicknesses up to 600 nm was achieved. After oxidation of the heating resistors, the membrane structure and contact holes were defined. The processing of the active chips was completed by electroplating of gold metal lines and back-side lithography. The valve seat at the passive chips, formed by RIE, had a height of about 10 μm . The anisotropic etching of both types of wafers was performed, time controlled, in a 25% TMAH solution.

The membrane thickness was determined by SEM measurements after dicing. The described microvalves had beam thicknesses around 12 μm . Completed valves were mounted on metallic transistor carriers (TO8) as shown in Fig. 9.

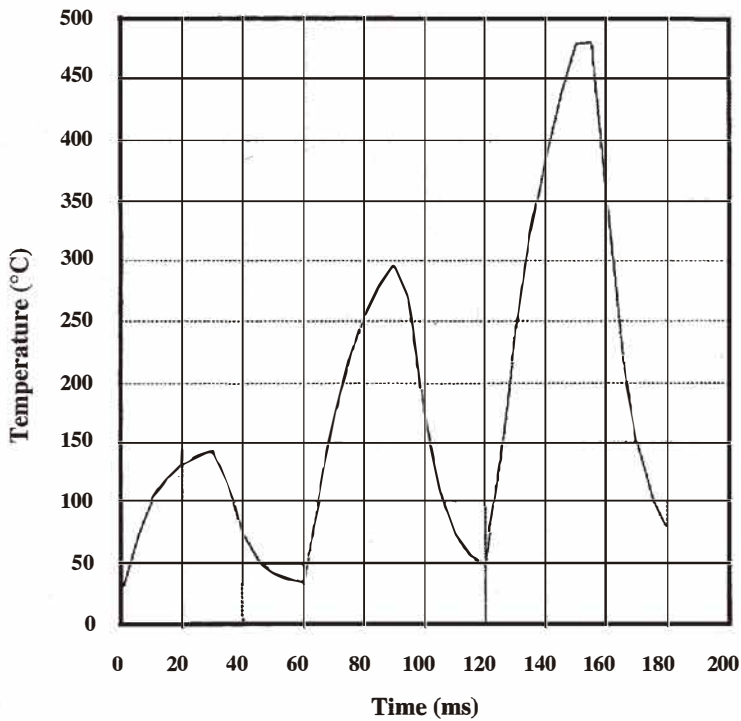


Fig. 7. Temperature in the center of the membrane vs. time for heating with successive pulses (30 ms on/30 ms off) of 1 W, 2W and 3W.

6. Results

The static gas flow and dynamic behavior were measured for different inlet pressures as a function of input power. Figure 10 shows typical flow characteristics (N_2) of a valve for different inlet pressures obtained at static measurement conditions.

For every input pressure, there is a certain power at which gas flow rises dramatically. In a small power range, a strong hysteresis effect could be observed. This behavior agrees with the theoretical considerations of a buckling mechanism. Before and after the buckling step, the gas flow rises slowly with increasing electrical power.

In the power range above the critical value further increase of the gas flow can be attributed to the continuing thermal expansion of the membrane. The switching of the valve above the critical power (*e.g.*, above 2.4 W at 0.5 bar) was accompanied by a characteristic snapping sound.

In the low-power range, the valves show a steep flow increase with values around 40 ml/min, far above the detection limit of the flowmeter used here. Similar to the main

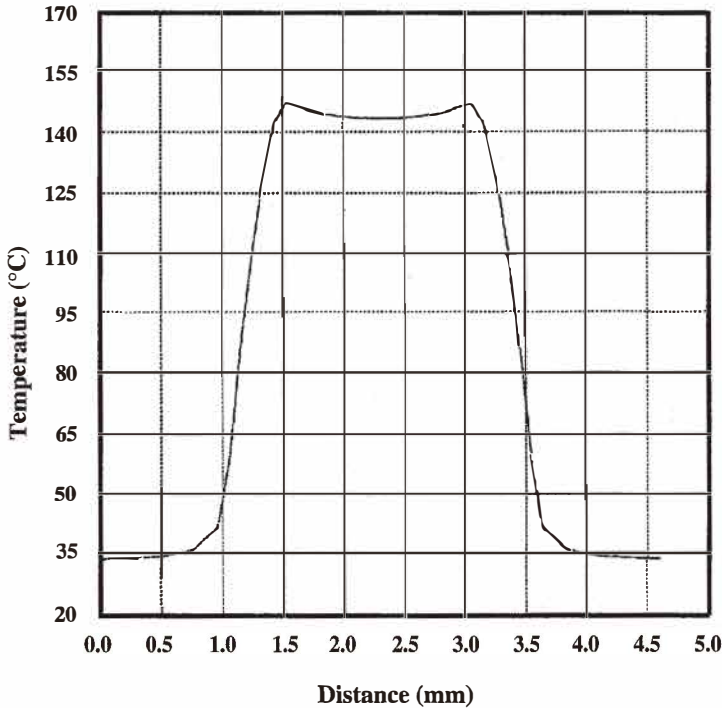


Fig. 8. Temperature distributions across the chip model after 30 ms heating with 1 W input power.

buckling step, a small hysteresis has been detected. This behavior can be explained by the initial buckling step which results in a wavy-shaped membrane, supported by the valve seat chip. Therefore, small gas flow through a partially free orifice (presumably at the edges) is possible.

Accuracy and reproducibility of the static flow measurements (rotameter) can be estimated to only about 20%. With heating of the entire device, the gas flow changes with time.

Figure 11 illustrates the dynamic behavior of a valve operated in a pulsed mode. The gas flow was determined with a fast mass flow controller connected to a digital oscilloscope. The switching voltage and the current flowing through the heaters were recorded simultaneously.

To characterize the response of a valve, three time constants have been used; t_{flow} is the time needed to reach maximum gas flow at given heating conditions; t_{on} corresponds to 10% of the average maximum value; t_{off} is the closing time of the valve. Figure 12 shows the change of the time constants as functions of the inlet pressure under constant heating conditions (1.8 W/ 100 ms power pulses at a frequency of 3.3 Hz). Up to a pressure of 0.6

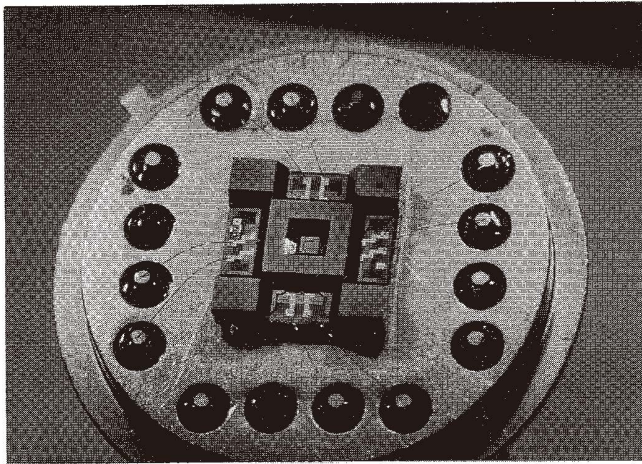


Fig. 9. Mounted microvalve.

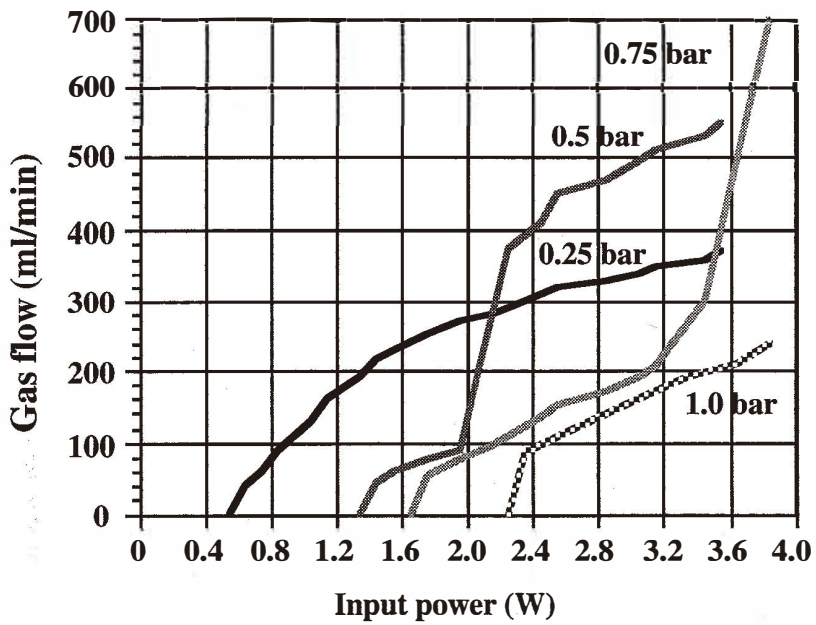


Fig. 10. Flow characteristics for a valve at different inlet pressures.

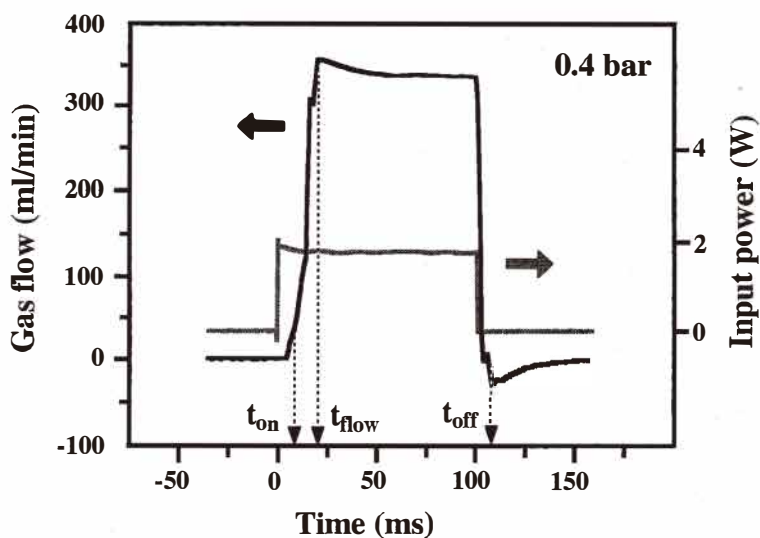


Fig. 11. One switching cycle of a valve operated with a 100 ms voltage pulse for 0.4 bar inlet pressure and 1.8 W power.

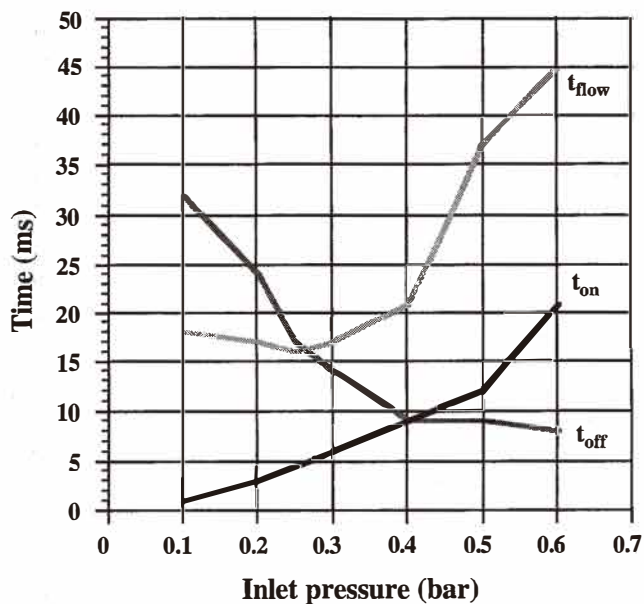


Fig. 12. Time constants vs. inlet pressure at constant heating conditions (1.8 W, 100 ms pulses, 3.3 Hz).

bar the valve begins to open within 20 ms. While t_{on} and t_{flow} rise with increasing input pressure, the closure time decreases because the pressure pushes the membrane downward. At a power of 3.6 W, the valves reach full gas flow within 20 ms under pressures up to 1.5 bar. Due to increased heating of the microvalve, power values above 1.5–2.0 W are useful only for short-term switching applications. All time values include the delay in the response of the mass flow controller (3 ms).

The measured response times are in a good agreement with the FEA calculations of the thermal behavior of the membrane structure for short heating pulses (30 ms). However the real measured maximum switching pressure is nearly 30–40% higher than predicted by FEA under the same heating conditions. For example, for an actual device heated with 1.2 W for 30 ms (and 3.3 Hz) flow can be detected at pressures up to 0.25 bar. Moreover, in the simulations, the cooling effect of the valve seat chip which lowers the membrane temperature significantly has not been considered. This behavior correlates to the assumption made above of an initial buckling step resulting in a wavy-shaped membrane contacting the valve seat chip. Figure 13 shows the full gas flow through a valve operated with 100 ms pulses at 1.8 W as a function of the inlet pressure.

Using the experimental setup shown in Fig. 14 the operation of pneumatic control systems with the microvalve as a pilot valve was tested. The inlet pressure p_0 (compressed air) is kept at a constant level during the switching process by a volume of 0.4 l. p_1 represents the pressure in a much smaller volume, connected to the outlet of the microvalve. The times when p_1 reaches 10% and 90% of p_0 are denoted by t_{10} and t_{90} , respectively (Table

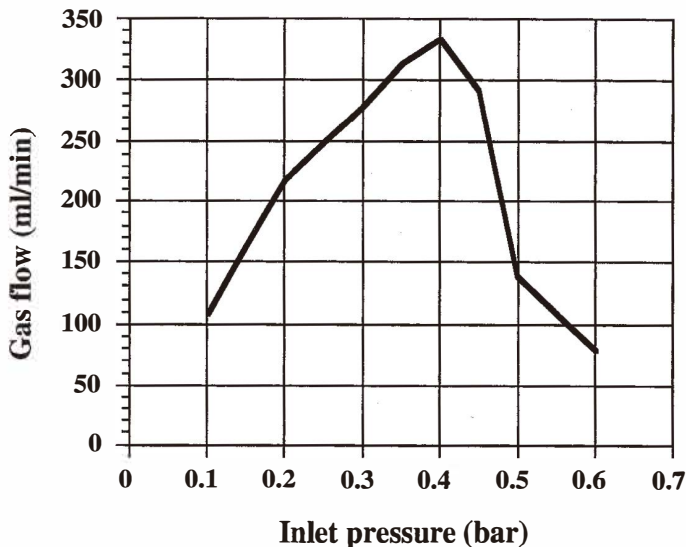


Fig. 13. Gas flow through a valve at constant heating conditions (1.8 W, 100 ms pulses, 3.3 Hz) as a function of the inlet pressure.

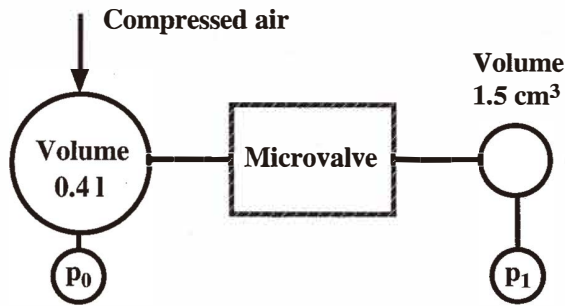


Fig. 14. Experimental setup for testing the valves in conditions which correspond to those of a pneumatic control system.

1). With an input power of 3.6 W the switching process is completed within 300 ms under pressures up to 1.0 bar. Due to the short switching time heating of the microvalve is relatively small.

The long-term stability of a valve is a very important factor for commercial application. A durability test was performed at a switching frequency of 3.3 Hz (100 ms on, 200 ms off) for 0.5 bar inlet pressure and 3 W input power. After every 500,000 cycles, test measurements of flow characteristics were performed. No degradation was observed after more than 2 million cycles. This indicates that frequent buckling of the membrane structure does not affect its mechanical stability.

7. Conclusions

A microvalve based on thermally induced buckling of a silicon beam structure has been developed and successfully operated. It has been demonstrated that the principle of thermal buckling is applicable to the fabrication of pneumatic valves with high flow rates and short switching times.

Table 1

Dynamic behavior of a pneumatic control system consisting of the microvalve and a small volume (Fig. 14).

p_0 , bar	t_{10} , ms	t_{90} , ms
0.25	5	200
0.50	7	200
0.75	14	250
1.00	17	275

A valve relying on buckling requires no metallization on the membrane itself. This allows for easy fabrication. Moreover, such a valve is not affected by the typical problems which are attributed to metallic layers. In particular, it is not subjected to thermally enhanced effects such as degradation or corrosion of the metal layer which deteriorate the valve performance and stability.

The power consumption of this first prototype is too high to be practical. However, it is believed that an optimized design can significantly increase the efficiency. Work is currently in progress with this aim.

References

- 1 M. A. Huff, J. R. Gilbert and M. A. Schmidt: Proc. Transducers '93, Yokohama, p. 98.
- 2 T. Ohnstein, T. Fukiura, J. Ridley and U. Bonne: Proc. MEMS '90, Napa Valley, p. 95.
- 3 H.-P. Trah, H. Baumann, C. Döring, H. Goebel, T. Grauer and M. Mettner: *Sensors and Actuators A* **39** (1993) 169.
- 4 S. Shoji, B. van der Schoot, N. de Rooji and M. Esashi: Proc. Transducers '91, San Francisco, p. 1052.
- 5 K. Yanagisawa, H. Kuwano and A. Tago: Proc. Transducers '93, Yokohama, p. 102.
- 6 B. Wagner and W. Benecke: Proc. MEMS '91, Nara, p. 27.
- 7 M. Shikida, K. Sato, S. Tanaka, Y. Kawamura and Y. Fujisaki: Proc. Transducers '93, Yokohama, p. 94.
- 8 J. Branebjerg and P. Gravesen: Proc. MEMS '92, Travemünde, p. 6.
- 9 H. Jerman: Proc. Transducers '91, San Francisco, p. 1045.
- 10 B. Hälg: *IEEE Transact. on Electron Devices* **37** (1990) 2230.
- 11 U. Lindberg, J. Söderkvist, T. Lammerink and M. Elwenspoek: Proc. Micro Mechanics Europe '93, Neuchatel, p. 115.